

Landau-type sudden transitions of quantum correlations

Mikhail A. Yurischev*

Institute of Problems of Chemical Physics of the Russian Academy of Sciences, 142432 Chernogolovka, Moscow Region, Russia

Sudden changes of quantum correlations in the Bell-diagonal states are well-known effects. They occur when the set of optimal parameters that determine the quantum correlation consists of isolated points and optimal parameters during the evolution of the system jump from one such point to another (e.g., the optimal measurement angle of the quantum discord changes discontinuously from zero to $\pi/2$ or vice versa). However, when considering more general X quantum states, we found that quantum discord and one-way quantum work deficit can experience sudden changes of other kinds. Namely, the optimal measurement angle may suddenly start to shift *continuously* from its stationary value 0 or $\pi/2$ to an intermediate optimal measurement angle $\vartheta \in (0, \pi/2)$. This leads to a new behavior of quantum correlations, which is mathematically described by the Landau phenomenological theory of second-order phase transitions. In addition, for the one-way quantum work deficit, we found cases where the optimal measurement angle jumps from zero to a nonzero step less than $\pi/2$, and then continuously changes its value. This behavior of quantum correlation is similar to a first-order phase transition in Landau's theory. Dependencies of quantum discord and one-way quantum work deficit near the boundaries, which separate regions with state-dependent (variable) and state-independent (stationary, constant) optimal measurement angles, are examined in detail on an example of the XXZ spin model in an external field at thermal equilibrium.

Keywords: Quantum discord, One-way quantum work deficit, Optimal measurement angle, Sudden changes

I. INTRODUCTION

Quantum correlations play a crucial role in quantum information science and technologies. Many types of these correlations have been introduced so far, and now their properties are carefully studied both theoretically and experimentally [1–3]. The most important among quantum correlations are quantum entanglement, discord, one-way quantum work deficit and some others [4].

Many quantitative measures of quantum correlations for the mixed states involve optimization procedure for the corresponding objective function or functional. For example, the entanglement of formation within the entanglement-separability paradigm [5] is defined as the minimized average entanglement over all ensembles of pure states realizing the given state [6]. Definitions of the quantum discord and one-way quantum work deficit contain minimizations, respectively, of conditional and post-measurement entropies over local measurements [7–9], see also [2].

Let $\Phi(p; x)$ be a continuous and smooth objective function, where p is the vector of optimization parameters and x represents additional variables, which do not participate in the optimization process but can deform the objective function. After optimization, one obtains the function $f(x) = \min_p \Phi(p; x)$. It is natural to expect that the optimal parameters, $\{p_{opt}\}$, depend continuously on the variables x at least near the given optimal point. However, it has long been noticed that the most practical constrained optimization problems in natural sciences

very often have an optimal solution at the boundaries: “Real life optimization problems often involves one or more constraints and in most cases, the optimal solutions to such problems lie on constraint boundaries” [10]. If the set of optimal points is countable (for example, when the constraints are one-dimensional segments with two endpoints each) and the above empirical observation holds true, then the resulting function $f(x)$ will be piecewise, consisting of analytic subfunctions (branches or phases, fractions – in physical language), each of which is defined in its own separate domain. The X quantum states are a relevant example of this; see Fig. 1 and details below.

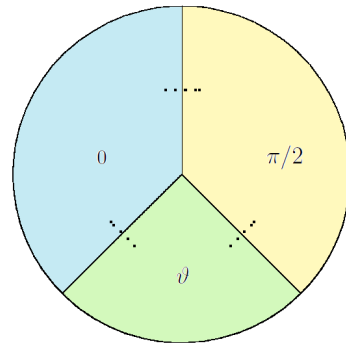


FIG. 1: (Color online) Domain of quantum discord and one-way quantum work deficit functions for the X states (schematically). Generally, it consists of three regions: with constant (0 and $\pi/2$) and variable (ϑ) optimal measurement angles. Dotted lines show paths crossing the boundaries. The transitions between 0- and $\pi/2$ -regions are simple jumps of optimal parameter, while transitions from 0- or $\pi/2$ - to ϑ -region correspond to the Landau-type sudden changes of the correlations.

*yur@itp.ac.ru

A similar picture takes place for entangled-untangled transitions, when in the course of evolution in time, temperature, etc., the optimal ensemble suddenly begins to lead to a separable state and quantum entanglement disappears in a non-zero area (volume) [11–16]. Next, according to the Luo formula [17], the quantum discord function of Bell-diagonal states, which are a special case of X quantum states, consist of branches that can be parametrized using the optimal measurement angles zero and $\pi/2$ [18]. It is important to emphasize that the corresponding domain does not contain regions with the variable optimal measurement angles and therefore transitions from one branch to another are simple jumps of optimal parameter. Such transitions have been classified as sudden changes and they are accompanied by fractures (sharp bends) on the curves of quantum correlation dependencies [19–23].

Further development of the theory was associated with the consideration of quantum discord in arbitrary X quantum states. The first attempt in this direction was made by Ali et al. [24]. Unfortunately, the authors decided that the extreme values of the parameters that determine von Neumann measurements, are reached only at the endpoints. However, shortly thereafter, counterexamples of X density matrices were given, which clearly demonstrated the minimum of the conditional entropy function inside the open interval, not at the endpoints of the optimization parameter segment [25, 26].

The next step was taken in Refs. [27–29], where it was shown that the set of interior optimal points form a separate continuous subregion with precise boundaries. Equations for such boundaries were proposed in the same papers [27–29]. Their solutions allowed to prove that the regions under discussion are small and narrow. Due to the presence of such regions, we are faced with exclusion from the above-mentioned empirical rule, since there is a return to the continuous dependence of the optimal parameter on variables that change the state of the system and, therefore, the corresponding objective function.

Then, similar regions with state-dependent optimal measurements were also found in the one-way quantum work deficit [30–32]. In Ref. [33], we proposed an optical setup scheme and performed numerical simulations that showed that the mysterious domain with variable optimal parameter may be detected experimentally using existing modern optical means.

This article is devoted to a detailed description of the behavior of quantum discord and one-way quantum work deficit in the vicinity of boundaries separating the regions with state-dependent and stationary (constant) optimal measurement angles. We take a two-qubit XXZ model in a homogeneous magnetic field at thermal equilibrium. This simple system already demonstrates the phenomena declared in the title of the paper. We show that quantum discord can undergo sudden changes that are surprisingly similar to the Landau continuous phase transitions. On the other hand, the behavior of the quantum work deficit is richer. This quantum correlation under certain condi-

tions exhibits sudden changes similar not only to second-order phase transitions, but also to the first-order ones.

This paper is organized as follows. The next section recalls the definitions of the one-way quantum work deficit and quantum discord. Model Hamiltonian and entropy expressions determining quantum correlations are presented in Sec. III. Sudden transitions of quantum work deficit and quantum discord are discussed in Secs. IV and V, respectively. Finally, Sec. VI provides a brief summary and concluding remarks.

II. PRELIMINARIES

Here we remember some definitions and well-known relations that will be needed in the following sections.

Let us start with the one-way quantum work deficit (or in short, work deficit) Δ , also sometimes referred to as “thermal discord” [2]. For a bipartite system AB in state ρ , it is defined as the minimum difference between the von Neumann entropies of the post- and pre-measurement states [9, 34, 35]:

$$\Delta = \min_{\{\Pi_k^B\}} S(\bar{\rho}) - S(\rho), \quad (1)$$

where local measurements are performed for definiteness on the subsystem B : $\Pi_k^B = \mathbb{I} \otimes \Pi_k$. In Eq. (1), $\bar{\rho} = \sum_k p_k \rho_k$ is the weighted average of post-measurement states

$$\rho_k = \frac{1}{p_k} (\mathbb{I} \otimes \Pi_k) \rho (\mathbb{I} \otimes \Pi_k)^\dagger \quad (2)$$

appearing, according to the Born rule, with probabilities $p_k = \text{Tr}(\Pi_k^B \rho \Pi_k^{B\dagger})$. It is noteworthy that the probabilities drop out from the state after measurement:

$$\bar{\rho} = \sum_k (\mathbb{I} \otimes \Pi_k) \rho (\mathbb{I} \otimes \Pi_k)^\dagger \quad (3)$$

what corresponds to nonselective measurement.

It is known [36] that generalized measurements can decrease entropy, but orthogonal projective ones do not. Therefore, when the work deficit measures are considered, ones use the projective measurements which satisfy to conditions $\Pi_k \Pi_l = \delta_{kl} \Pi_k$. For a binary system, $\Pi_k = V \pi_k V^\dagger$ ($k = 0, 1$) with $\pi_k = |k\rangle\langle k|$ and transformations $\{V\}$ belonging to the special unitary group SU_2 . Such transformations can be parametrized by rotations

$$V(\theta, \phi) = \begin{pmatrix} \cos \frac{\theta}{2} & -e^{-i\phi} \sin \frac{\theta}{2} \\ e^{i\phi} \sin \frac{\theta}{2} & \cos \frac{\theta}{2} \end{pmatrix}, \quad (4)$$

where $\theta \in [0, \pi]$ and $\phi \in [0, 2\pi)$ are the polar and azimuthal angles, respectively.

Similarly, the definition of quantum discord Q for a composite system AB can be written as the minimum

discrepancy between the two quantum versions of conditional entropy. On the one hand, there is a formally-defined quantum analogue of classical conditional entropy that is given as

$$S(A|B) = S(\rho) - S(\rho_B), \quad (5)$$

where $\rho_B = \text{Tr}_A \rho$ is the reduced quantum state of subsystem B . On the other hand, the average measurement-based quantum conditional entropy was motivated to be given by [37]

$$\bar{S} \equiv S(A|\{\Pi_k^B\}) = \sum_k p_k S(\rho_{A|k}), \quad (6)$$

where

$$\rho_{A|k} = \frac{1}{p_k} \text{Tr}_B[(\mathbf{I} \otimes \Pi_k) \rho (\mathbf{I} \otimes \Pi_k)^\dagger] \quad (7)$$

is the conditional state of subsystem A after obtaining the outcome k on the subsystem B . Now the quantum discord is written as [2, 35]

$$Q = \min_{\{\Pi_k^B\}} S(A|\{\Pi_k^B\}) - S(A|B). \quad (8)$$

For the quantum discord, we also restrict ourselves to the orthogonal projective measurements (von Neumann measurements).

In the case of projective measurements, the measurement-based conditional entropy and the entropy of post-measured state are related to each other through the condition [38, 39]

$$S(A|\{\Pi_k^B\}) = S(\bar{\rho}) - S(\bar{\rho}_B), \quad (9)$$

where $\bar{\rho}$ is given by Eq. (3) and $\bar{\rho}_B = \text{Tr}_A \bar{\rho}$ is the state of party B after the measurement. Note that the right side of Eq. (9) is similar to the right side of formally-defined quantum conditional entropy (5). Equation (9) allows actually compute the average measurement-based conditional entropy.

III. HAMILTONIAN AND ENTROPY FUNCTIONS

Consider a system of two spins 1/2 in a uniform magnetic field B with the Hamiltonian

$$H = -\frac{1}{2}[J(\sigma_1^x \sigma_2^x + \sigma_1^y \sigma_2^y) + J_z \sigma_1^z \sigma_2^z] - \frac{1}{2}B(\sigma_1^z + \sigma_2^z), \quad (10)$$

where J and J_z are the coupling constants and σ_j^x , σ_j^y , and σ_j^z the Pauli spin matrices at sites $j = 1, 2$. Note that there are a large number of dimeric and quasidimeric magnetic materials similar to this system, in which quantum correlations are intensively studied experimentally [2, 3].

The energy levels of the Hamiltonian (10) are given as

$$E_{1,2} = -\frac{1}{2}J_z \pm B, \quad E_{3,4} = \frac{1}{2}J_z \pm J \quad (11)$$

and hence the partition function $Z = \sum_i \exp(-E_i/T)$ equals

$$Z = 2 \left(e^{J_z/2T} \cosh \frac{B}{T} + e^{-J_z/2T} \cosh \frac{J}{T} \right), \quad (12)$$

where T is the absolute temperature in energy units. The function $Z(T, B)$ is invariant under substitutions of both $J \rightarrow -J$ and $B \rightarrow -B$.

A. Pre-measurement entropies

The free energy (Helmholtz thermodynamic potential) is equal to $F(T, B) = -T \ln Z$ and, therefore, the usual thermodynamic entropy $S = -\partial F/\partial T$ is expressed for the system (10) by the equation

$$\begin{aligned} S(T, B) = & -\frac{1}{Z} \left[\frac{B + J_z/2}{T} \exp\left(\frac{B + J_z/2}{T}\right) \right. \\ & - \frac{B - J_z/2}{T} \exp\left(-\frac{B - J_z/2}{T}\right) \\ & + \frac{J - J_z/2}{T} \exp\left(\frac{J - J_z/2}{T}\right) \\ & \left. - \frac{J + J_z/2}{T} \exp\left(-\frac{J + J_z/2}{T}\right) \right] + \ln Z \quad (13) \end{aligned}$$

with Z equals (12). From here one can obtain the heat capacity $C(T, B) = T \partial S/\partial T$.

The Gibbs density operator $\rho = \exp(-H/T)/Z$ has a block-diagonal structure, which is a special case of the X-matrix:

$$\begin{aligned} \rho = & \begin{pmatrix} a & 0 & 0 & 0 \\ 0 & b & v & 0 \\ 0 & v & b & 0 \\ 0 & 0 & 0 & d \end{pmatrix} = \frac{1}{4}[1 + s_1(\sigma_1^z + \sigma_2^z) \\ & + c_1(\sigma_1^x \sigma_2^x + \sigma_1^y \sigma_2^y) + c_3 \sigma_1^z \sigma_2^z], \quad (14) \end{aligned}$$

where the unary and binary statistical correlations equal

$$s_1 = a - d, \quad c_1 = 2v, \quad c_3 = a - 2b + d. \quad (15)$$

The entries of matrix ρ are given as

$$a = \frac{1}{Z} \exp[(J_z/2 + B)/T], \quad b = \frac{1}{Z} e^{-J_z/2T} \cosh(J/T), \quad (16)$$

$$d = \frac{1}{Z} \exp[(J_z/2 - B)/T], \quad v = \frac{1}{Z} e^{-J_z/2T} \sinh(J/T)$$

with the normalization condition $a + 2b + d = 1$. The eigenvalues of the density matrix (14) are

$$\lambda_1 = a, \quad \lambda_{2,3} = b \pm v, \quad \lambda_4 = d \quad (17)$$

or

$$\begin{aligned}\lambda_{1,4} &= \frac{1}{Z} \exp[(J_z/2 \pm B)/T], \\ \lambda_{2,3} &= \frac{1}{Z} \exp[-(J_z/2 \pm J)/T].\end{aligned}\quad (18)$$

In accord with (17), the von Neumann entropy before measurement is equal to

$$\begin{aligned}S(\rho) &\equiv -\text{Tr}\rho \ln \rho = -\sum_i^4 \lambda_i \ln \lambda_i \\ &= -a \ln a - d \ln d - (b+v) \ln(b+v) - (b-v) \ln(b-v).\end{aligned}\quad (19)$$

(Here entropy is measured in nats; to convert this value

to bits, one should divide it by $\ln 2$.) After inserting expressions for a , b , d and v , the relation (19) returns to Eq. (13).

Similarly, the entropy of the reduced quantum state ρ_B is given as

$$S(\rho_B) = -(a+b) \ln(a+b) - (b+d) \ln(b+d). \quad (20)$$

Equations (19) and (20) allow to obtain quantum pseudo-conditional entropy (5).

B. Post-measurement entropies

Using relations from Sec. II and Eq. (14), we get the state of the system after measurement:

$$\bar{\rho} = \begin{pmatrix} \frac{a+b}{2} + \frac{a-b}{2} \cos^2 \theta & \cdot & \cdot & \cdot \\ \frac{a-b}{4} e^{i\phi} \sin 2\theta & b + \frac{a-b}{2} \sin^2 \theta & \cdot & \cdot \\ \frac{v}{4} e^{i\phi} \sin 2\theta & \frac{v}{2} \sin^2 \theta & b - \frac{b-d}{2} \sin^2 \theta & \cdot \\ \frac{v}{2} e^{2i\phi} \sin^2 \theta & -\frac{v}{4} e^{i\phi} \sin 2\theta & \frac{b-d}{4} e^{i\phi} \sin 2\theta & \frac{b+d}{2} - \frac{b-d}{2} \cos^2 \theta \end{pmatrix} \quad (21)$$

(in the upper triangular part, the dots have been put instead of the complex-conjugated entries of this Hermitian matrix).

Using, e.g., the package Mathematica one can prove that the invariants of matrix (21) do not contain the azimuthal angle ϕ , therefore, the eigenvalues of this matrix depend only on the polar angle θ . Moreover, the secular equation $\det(\bar{\rho} - \Lambda) = 0$ is factorized into product of two polynomials of second degree. This allows to get the eigenvalues of post-measurement state $\bar{\rho}$:

$$\Lambda_{1,2} = \frac{1}{4} [1 + (a-d) \cos \theta \pm \{[a-d + (1-4b) \cos \theta]^2 + 4v^2 \sin^2 \theta\}^{1/2}], \quad (22)$$

$$\Lambda_{3,4} = \frac{1}{4} [1 - (a-d) \cos \theta \pm \{[a-d - (1-4b) \cos \theta]^2 + 4v^2 \sin^2 \theta\}^{1/2}].$$

Hence, the post-measurement entropy is given as

$$\begin{aligned}\tilde{S}(\theta; T, B) &\equiv S(\bar{\rho}) = 2 \ln 2 \\ &- \frac{1}{4} \sum_{m,n=0}^1 \left[1 + (-1)^m (a-d) \cos \theta \right. \\ &\quad \left. + (-1)^n \sqrt{[a-d + (-1)^m (1-4b) \cos \theta]^2 + 4v^2 \sin^2 \theta} \right] \\ &\quad \times \ln \left[1 + (-1)^m (a-d) \cos \theta \right. \\ &\quad \left. + (-1)^n \sqrt{[a-d + (-1)^m (1-4b) \cos \theta]^2 + 4v^2 \sin^2 \theta} \right].\end{aligned}\quad (23)$$

The state of subsystem B after the measurement is equal to

$$\bar{\rho}_B = \begin{pmatrix} \frac{1}{2}(1 + \cos^2 \theta)a + b + \frac{1}{2}d \sin^2 \theta & \frac{1}{4}e^{-i\phi} \sin 2\theta \\ \frac{1}{4}e^{i\phi} \sin 2\theta & \frac{1}{2}a \sin^2 \theta + b + \frac{1}{2}(1 + \cos^2 \theta)d \end{pmatrix}. \quad (24)$$

Entropy of this state is given as

$$\begin{aligned}S(\bar{\rho}_B) &= \ln 2 - \frac{1}{2} \{ [1 + (a-d) \cos \theta] \ln [1 + (a-d) \cos \theta] \\ &\quad + [1 - (a-d) \cos \theta] \ln [1 - (a-d) \cos \theta] \},\end{aligned}\quad (25)$$

which also does not depend on ϕ .

Both entropies $S(\bar{\rho})$ and $S(\bar{\rho}_B)$ as functions of the argument θ are invariant under the transformation $\theta \rightarrow \pi - \theta$ and therefore this variable can be limited to the values of $\theta \in [0, \pi/2]$. It is easy to check by direct calculations that

$$\left. \frac{\partial S(\bar{\rho})}{\partial \theta} \right|_{\theta=0, \pi/2} = 0, \quad \left. \frac{\partial S(\bar{\rho}_B)}{\partial \theta} \right|_{\theta=0, \pi/2} = 0 \quad (26)$$

for any a, b, d , and v .

C. Conditional entropy

Equations (6), (9), (23), and (25) allow to get the conditional entropy function

$$\begin{aligned} \bar{S}(\theta; T, B) &= \tilde{S}(\theta; T, B) \\ &+ \frac{1 + (a-d)\cos\theta}{2} \ln \frac{1 + (a-d)\cos\theta}{2} \\ &+ \frac{1 - (a-d)\cos\theta}{2} \ln \frac{1 - (a-d)\cos\theta}{2} \end{aligned} \quad (27)$$

with quantities a and d equal to the relations (16).

Finally, according to Eq. (26), the first derivatives of the post-measurement and conditional entropies with respect to the measurement angle θ vanish at boundaries,

$$\tilde{S}'(\theta; T, B)|_{\theta=0, \pi/2} = 0, \quad \bar{S}'(\theta; T, B)|_{\theta=0, \pi/2} = 0, \quad (28)$$

and therefore both endpoints $\theta = 0$ and $\pi/2$ are stationary (critical) and candidates for the global extrema.

So, the necessary equations are written down, and now we can proceed directly to the study of the behavior of quantum correlations.

IV. SUDDEN TRANSITIONS OF WORK DEFICIT

As applied to the model under discussion, the one-way quantum work deficit is given as

$$\Delta(T, B) = \min_{\vartheta} \Delta(\vartheta; T, B) \quad (29)$$

with non-optimized work deficit function

$$\Delta(\vartheta; T, B) = \tilde{S}(\vartheta; T, B) - S(T, B), \quad (30)$$

where $\tilde{S}(\vartheta; T, B)$ is expressed by Eq. (23) and $S(T, B)$ is given by (13); here ϑ is the current non-optimized measurement angle (the optimal measurement angle is denoted as ϑ). Note that the derivative of the work deficit with respect to temperature is proportional to the difference between heat capacity after (\tilde{C}) and before (C) optimal measurement:

$$T \frac{\partial \Delta}{\partial T} = \tilde{C}(T, B) - C(T, B). \quad (31)$$

This relationship points to a way to experimentally measure work deficit. Indeed, it is necessary to measure the specific heat before and after the measurement, and then integrate their difference normalized to temperature.

Using Eq. (30) we get the value of work deficit at the endpoint $\theta = 0$:

$$\begin{aligned} \Delta_0(T, B) &\equiv \Delta(0; T, B) \\ &= \frac{2}{Z} \left[\frac{J}{T} \sinh \frac{J}{T} - \ln \left(\cosh \frac{J}{T} \right) \cosh \frac{J}{T} \right] e^{-J_z/2T}. \end{aligned} \quad (32)$$

Its high-temperature asymptotics is

$$\Delta_0(T, B) = \frac{1}{4} \frac{J^2}{T^2} - \frac{1}{8} \frac{J_z J^2}{T^3} - \frac{1}{16} \frac{J^2(B^2 + J^2)}{T^4} + O\left(\frac{1}{T^5}\right). \quad (33)$$

At the second endpoint $\theta = \pi/2$, work deficit is equal to

$$\begin{aligned} \Delta_{\pi/2}(T, B) &\equiv \Delta(\pi/2; T, B) = \ln 2 - \frac{1+r}{2} \ln \frac{1+r}{2} \\ &- \frac{1-r}{2} \ln \frac{1-r}{2} - S(T, B), \end{aligned} \quad (34)$$

where

$$r = \frac{2}{Z} \left[e^{J_z/T} \sinh^2 \frac{B}{T} + e^{-J_z/T} \sinh^2 \frac{J}{T} \right]^{1/2}. \quad (35)$$

High-temperature expansion reads

$$\Delta_{\pi/2}(T, B) = \frac{1}{8} \frac{J^2 + J_z^2 + B^2}{T^2} + \frac{1}{8} \frac{J_z(B^2 - J^2)}{T^3} + O\left(\frac{1}{T^4}\right). \quad (36)$$

Comparing the main terms of the expansions (33) and (36), we conclude that for $T \rightarrow \infty$ the deficit will be determined by the Δ_0 -branch, if $J_z^2 + B^2 > J^2$, and by $\Delta_{\pi/2}$, if $J_z^2 + B^2 < J^2$.

It is clear that the one-way quantum work deficit (29) can be written as a choice of three alternative branches (phases):

$$\Delta = \min\{\Delta_0, \Delta_{\pi/2}, \Delta_{\vartheta}\}, \quad (37)$$

where Δ_0 and $\Delta_{\pi/2}$ are given by Eqs. (32) and (34) respectively, while Δ_{ϑ} is the amount of work deficit at the internal optimal point $\vartheta \in (0, \pi/2)$, if, of course, it exists there.

To further investigate the problem, we will use phase diagrams for the model that were obtained in the three-dimensional space (s_1, c_1, c_3) [32] and in the plane (T, B) for different values of J and J_z [40]. Phase diagrams consist of two regions with fixed optimal measurement angles (0 and $\pi/2$) and one region with variable, state-dependent optimal measurement angle ϑ . Boundary between Δ_0 and $\Delta_{\pi/2}$ phases is given by equation $\Delta_0 = \Delta_{\pi/2}$. Crossing this boundary leads to the usual sudden

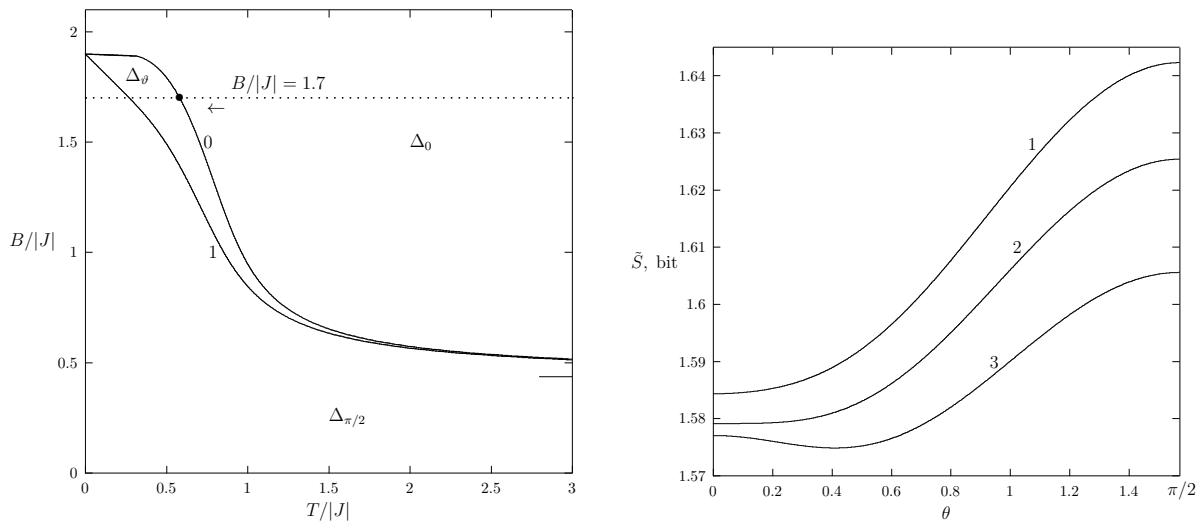


FIG. 2: (left panel) Temperature-field phase diagram of work deficit for the model with $J_z/|J| = -0.9$. Solid lines 0 and 1 are the 0- and $\pi/2$ -boundaries, respectively. Dotted straight line is the path of system evolution. The arrow shows the direction of evolution along the path. Black circle (\bullet) has coordinates $(0.58264, 1.7)$ and marks a crossing point of the path and 0-boundary curve. A long horizontal bar on the right ordinate axis marks the level that corresponds to the asymptote $B/|J| = 0.43589$. (right panel) Post-measurement entropy \tilde{S} vs measurement angle θ for $B/|J| = 1.7$ and $T/|J| = 0.65$ (1), 0.5826437 (2), 0.5 (3). The curve 3 has an interior minimum $\tilde{S}_{min} = 1.57487$ bit at $\theta_{min} = 0.40953 \approx 23.5^\circ$.

changes that were mentioned in Introduction and which are not discussed in our article. We are interested in transitions to the region Δ_θ . For the work deficit, as announced above, they can be of two types: (i) continuous and (ii) a relatively small ($< \pi/2$) jump of the optimal measurement angle and then continuous change of ϑ . We will study these two cases separately.

A. Continuous transitions

In the case under question, the post-measurement entropy $\tilde{S}(\theta)$ [and therefore the unoptimized work deficit $\Delta(\theta)$] has one internal minimum – inside the interval $(0, \pi/2)$. The 0- and $\pi/2$ -boundaries of the Δ_θ region are determined by the conditions, where the second derivatives of $\Delta(\theta)$ or, the same, $\tilde{S}(\theta)$ with respect to the mea-

surement angle θ vanish, respectively, at $\theta = 0$ and $\pi/2$ [31]:

$$\Delta''(0; T, B) = 0 \quad \text{and} \quad \Delta''(\pi/2; T, B) = 0 \quad (38)$$

or

$$\tilde{S}''(0; T, B) = 0 \quad \text{and} \quad \tilde{S}''(\pi/2; T, B) = 0. \quad (39)$$

These equations are based on the observation that the interior minimum of unimodal differentiable function in the closed interval with the zero first derivatives at endpoints appears or annihilates at the boundaries.

For the second derivatives at endpoints, $\tilde{S}''_0(T, B) \equiv \tilde{S}''(0; T, B)$ and $\tilde{S}''_{\pi/2}(T, B) \equiv \tilde{S}''(\pi/2; T, B)$, calculations yield

$$\begin{aligned} \tilde{S}''_0(T, B) = & \frac{1}{Z} \left[\left\{ \frac{B}{T} \sinh \frac{B}{T} + \left(\cosh \frac{B}{T} - e^{-J_z/T} \cosh \frac{J}{T} \right) \left[\frac{J_z}{T} - \ln \left(\cosh \frac{J}{T} \right) \right] \right\} e^{J_z/2T} \right. \\ & \left. - \frac{1}{2} e^{-J_z/2T} \left[\frac{(J_z + B)/T - \ln(\cosh(J/T))}{\exp((J_z + B)/T) - \cosh(J/B)} + \frac{(J_z - B)/T - \ln(\cosh(J/T))}{\exp((J_z - B)/T) - \cosh(J/B)} \right] \sinh^2 \frac{J}{T} \right] \end{aligned} \quad (40)$$

and

$$\begin{aligned} \tilde{S}''_{\pi/2}(T, B) = & 8v^2 \frac{ab + bd - ad - b^2 + v^2}{r^3} \ln \frac{1+r}{1-r} \\ & - \frac{1}{2} (a-d)^2 \left\{ \frac{[1 + (1-4b)/r]^2}{1+r} + \frac{[1 - (1-4b)/r]^2}{1-r} \right\}, \end{aligned} \quad (41)$$

where r is given, as before, by Eq. (35).

High-temperature expansions of functions (40) and

(41) are given as

$$\tilde{S}_0''(T, B)|_{T \rightarrow \infty} = \frac{J_z^2 - J^2 + B^2}{4T^2} + \frac{J_z B^2}{4T^3} + O(1/T^4) \quad (42)$$

and

$$\tilde{S}_{\pi/2}''(T, B)|_{T \rightarrow \infty} = \frac{J^2 - J_z^2 - B^2}{4T^2} - \frac{J_z B^2}{4T^3} + O(1/T^4). \quad (43)$$

Equating to zero the leading terms of these expansions, we get, in accord with (39), the equation of the asymptote for both boundaries:

$$B/|J| = \sqrt{1 - (J_z/J)^2}. \quad (44)$$

This result is useful for numerical estimates.

As an example, consider a system with coupling constants $J = \pm 1$ and $J_z = -0.9$. Using Eqs. (39)-(41) we find the 0- and $\pi/2$ -boundaries. The corresponding phase diagram in the plane (T, B) is shown in Fig. 2, left. When $T \rightarrow \infty$, curves 0 and 1 tend as predicted Eq. (44) to the horizontal asymptote $B/|J| = 0.43589$.

Consider the path $B/|J| = 1.7$. It intersects the 0- and $\pi/2$ -boundaries respectively at the points $T_0/|J| = 0.58264$ and $T_{\pi/2}/|J| = 0.27228$ (see again Fig. 2, left). This allows us to estimate the size (width) of the region Δ_ϑ as $(T_0 - T_{\pi/2})/[(T_0 + T_{\pi/2})/2] = 0.72612 \approx 72.6\%$. Thus, in the temperature-field coordinates, the width of the region with a variable angle of optimal measurement is large. This contrasts with the sizes of Δ_ϑ -regions in the space (s_1, c_1, c_3) , where they are tiny and narrow [32].

The behavior of post-measured entropy \tilde{S} versus the measurement angle θ is shown in Fig. 2, right. When temperatures are high enough, the curves have a minimum at the endpoint $\theta = 0$. However, as the system cools, this minimum flattens, its behavior changes from law $\sim \theta^2$ to $\sim \theta^4$ at $T_0/|J| = 0.5826437$ (curve 2). With a further decrease in temperature, an internal minimum appears on the curve $\tilde{S}(\theta)$, and the spin system continuously enters in the region Δ_ϑ with the variable optimal measurement angle $\vartheta > 0$. This behavior is similar to the continuous phase transition of Landau's theory [41, 42].

The function $\tilde{S}(\theta)$ is even and its expansion in a Taylor series at $\theta = 0$ has the form

$$\tilde{S}(\theta; T, B) = \tilde{S}_0(T, B) + \frac{1}{2!} \tilde{S}_0''(T, B) \theta^2 + \frac{1}{4!} \tilde{S}_0''''(T, B) \theta^4 + \dots, \quad (45)$$

where $\tilde{S}_0(T, B)$ equals $\tilde{S}(0; T, B)$, $\tilde{S}_0''(T, B)$ is given by Eq. (40), and $\tilde{S}_0''''(T, B)$ is the fourth derivative of post-measurement entropy with respect to the measurement angle at $\theta = 0$. Hence the expansion of work deficit has the form

$$\tilde{\Delta}(\theta; T, B) = \Delta_0(T, B) + \frac{1}{2!} \tilde{S}_0''(T, B) \theta^2 + \frac{1}{4!} \tilde{S}_0''''(T, B) \theta^4 + \dots, \quad (46)$$

where $\Delta_0(T, B)$ is given by Eq. (32). These series are similar to the Landau expansion of the thermodynamic

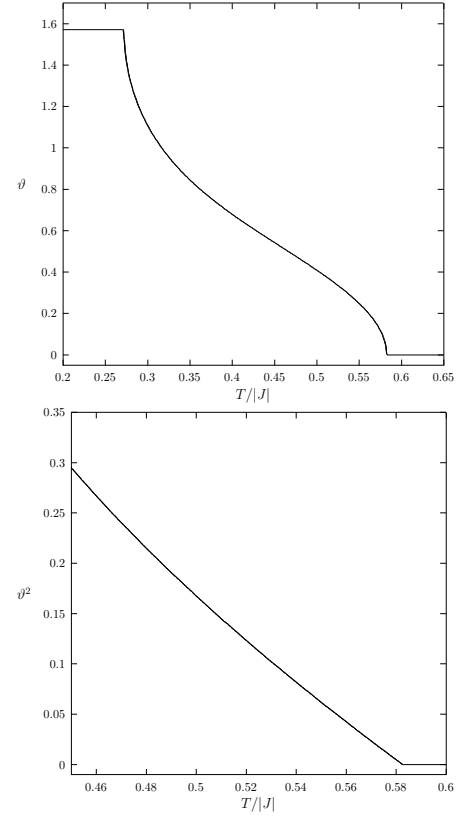


FIG. 3: Optimal measurement angle ϑ (top) and its square (bottom) as functions of temperature by $J_z/|J| = -0.9$ and $B/|J| = 1.7$.

potential (Gibbs free energy) in his theory of second-order phase transitions [41, 42]. In our problem, $\tilde{S}(\theta)$ or $\Delta(\theta)$ play a role of the thermodynamic potential and the optimal measurement angle ϑ is a counterpart of Landau's order parameter. The vanishing of the coefficient at the quadratic term corresponds to the sudden transition point.

The temperature dependence of ϑ is shown in Fig. 3, top. The optimal measurement angle takes constant values $\vartheta = 0$ or $\vartheta = \pi/2$ for $T \geq T_0 = 0.58264|J|$ and $T \leq T_{\pi/2} = 0.27228|J|$, respectively. In the intermediate region, the angle $\vartheta(T)$ is a continuous and smooth function that monotonically changes from zero to the maximum possible value $\pi/2$. The square of the optimal measurement angle $\vartheta^2(T)$ varies linearly in the region $0 \leq (T_0 - T)/T_0 \ll 1$, as can be seen from Fig. 3, bottom. Thus,

$$\vartheta(T) = \begin{cases} A \cdot (T_0 - T)^\beta, & \text{if } T < T_0 \\ 0, & \text{if } T \geq T_0, \end{cases} \quad (47)$$

where the critical exponent $\beta = 1/2$ and the singularity amplitude $A \approx 1.37$, taking into account that $|J| = 1$. This power-law behavior belongs to the mean-field universality class of criticality.

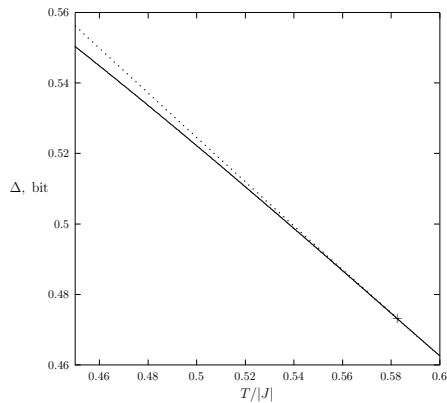


FIG. 4: Optimized work deficit Δ (solid line) and branch Δ_0 (dotted line) upon temperature by $J_z/|J| = -0.9$ and $B/|J| = 1.7$. The symbol “plus” has coordinates (0.58264, 0.47309) and marks the split point of these two curves.

When the system further evolves along the path $B/|J| = 1.7$, quantum correlation Δ undergoes a new sudden transition, similar to a second-order phase transition, at the temperature $T_{\pi/2} = 0.27228|J|$. Post-measurement entropy is approximated near this point by expansion

$$\begin{aligned} \tilde{S}(\theta; T, B) &= \tilde{S}_{\pi/2}(T, B) + \frac{1}{2!} \tilde{S}''_{\pi/2}(T, B) \cdot (\theta - \pi/2)^2 \\ &\quad + \frac{1}{4!} \tilde{S}''''_{\pi/2}(T, B) \cdot (\theta - \pi/2)^4 + \dots, \end{aligned} \quad (48)$$

where $\tilde{S}_{\pi/2}(T, B) = \tilde{S}(\pi/2; T, B)$, $\tilde{S}''_{\pi/2}(T, B)$ equals (41), and $\tilde{S}''''_{\pi/2}(T, B)$ is the fourth-order derivative of $\tilde{S}(\theta)$ at $\theta = \pi/2$. Here, the inner minimum reaches a maximum at the endpoint $\theta = \pi/2$ and merges with him. The optimal measurement angle will then remain constant at $\pi/2$, up to absolute zero temperature; see Fig. 3, top.

Further, the temperature behavior of the optimized one-way quantum work deficit $\Delta_{\vartheta}(T, B)$ near the critical temperature T_0 is shown in Fig. 4 by solid line. The dependence $\Delta_0(T, B)$ drawn with a dotted line is shown for comparison. Both curves exactly coincide in the temperature region $T \geq T_0 = 0.58264$. However the behavior of these functions becomes different for $T < T_0$ – after the point marked with “+” in Fig. 4. The error introduced by the Δ_0 reaches 1.04% at $T/|J| = 0.45$.

Dependence of Δ on temperature in Fig. 4 looks like a continuous and smooth function. However, this picture breaks down when going to derivatives. The first derivative of Δ with respect to temperature is continuous but exhibits a fracture at $T = T_0$ (see the solid line in Fig. 5, top). From this we can conclude that the work deficit refers to the functions of differentiability class C^1 . At the same time, the derivative of the function $\Delta_0(T)$ (dotted line) remains continuous and smooth. Moreover, the second derivative of Δ has discontinuity at $T = T_0$

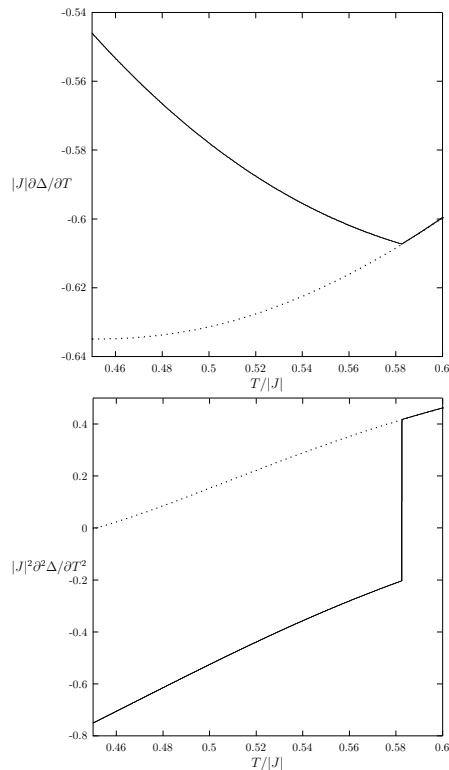


FIG. 5: The first (top) and second (bottom) derivatives of the optimized work deficit Δ (solid lines) and branch Δ_0 (dotted lines) depending on temperature by $J_z/|J| = -0.9$ and $B/|J| = 1.7$.

(solid line in Fig. 5, bottom) and therefore the behavior of work deficit here is similar to the behavior in a second-order phase transition. This is in complete analogy with the Landau theory [42–44] and Ehrenfest classification of phase transitions [45].

B. Discontinuous-continuous combined transitions

It is remarkable that the post-measurement entropy as a function of the measurement angle may show more complex behavior than unimodal. Namely, it can have two extrema (one minimum and one maximum) inside the open interval $(0, \pi/2)$, i.e. exhibit bimodal dependence [31]. This behavior is described by the sixth-order Taylor expansion

$$\tilde{S}(\theta; T, B) - \tilde{S}_0(T, B) \propto \alpha_1 \theta^2 + \alpha_2 \theta^4 + \theta^6, \quad (49)$$

where α_i ($i = 1, 2$) are the reduced expansion coefficients. This leads to a qualitatively new type of sudden transitions.

Consider the model with coupling $J_z/|J| = -1.5$. The corresponding phase diagram is shown in Fig. 6, left. The boundary lines here do not go to infinity, which is consistent with prediction (44).

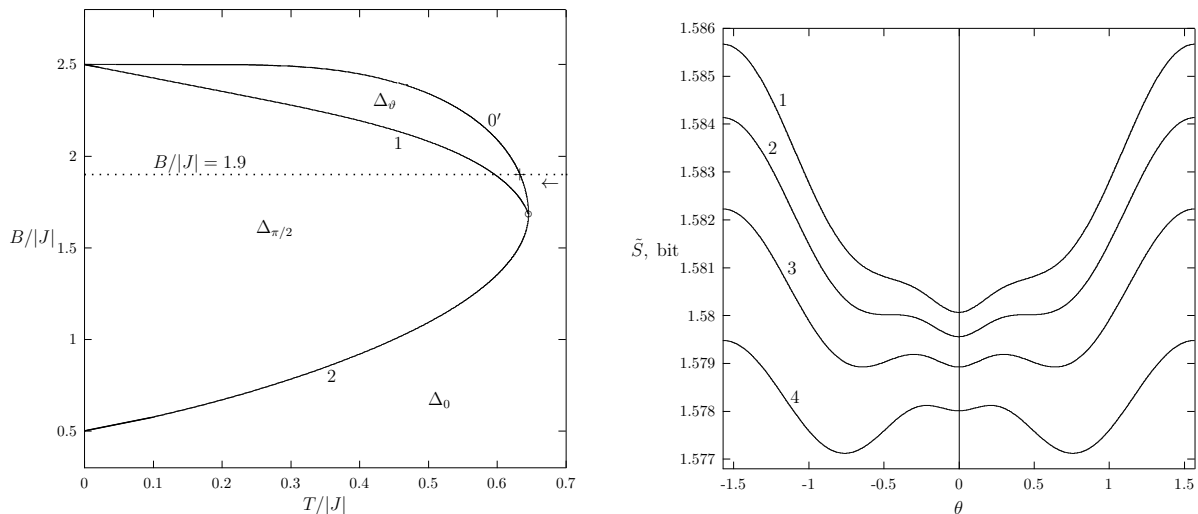


FIG. 6: (left panel) Temperature-field phase diagram of work deficit for the model with $J_z/|J| = -1.5$. Solid lines $0'$ and 1 are the $0'$ - and $\pi/2$ -boundaries, respectively; solid line 2 is the boundary between the phases Δ_0 and $\Delta_{\pi/2}$. Dotted straight line is the path of system evolution. The arrow shows the direction of evolution along the path. The “+” symbol has coordinates $(0.63329, 1.9)$ and marks an intersection point of the path and $0'$ -boundary. (right panel) Post-measurement entropy \tilde{S} vs measurement angle θ for $B/|J| = 1.9$ and $T/|J| = 0.64$ (1), 0.637 (2), 0.63329 (3), and 0.628 (4).

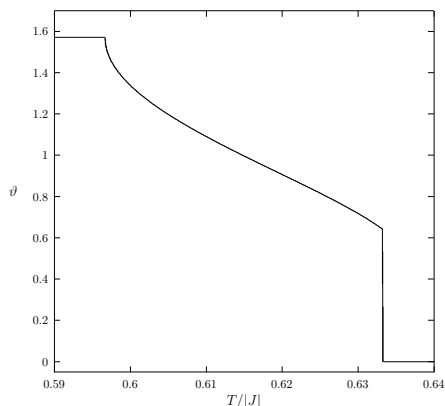


FIG. 7: Optimal measurement angle ϑ versus temperature for the coupling $J_z/|J| = -1.5$ and external field $B/|J| = 1.9$. The jump $\Delta\vartheta = 0.64026 \approx 36.7^\circ$ occurs at the temperature $T_{c,0} = 0.63329|J|$.

Let the system evolve along the trajectory $B/|J| = 1.9$ towards lower temperatures. In this case, the shape of post-measurement entropy will be deformed, as shown in Fig. 6, right. (In order to improve clarity, this figure is presented in a wider window $[-\pi/2, \pi/2]$.) At a sufficiently high temperature, the dependence $\tilde{S}(\theta)$ is a monotonically increasing function in the interval $[0, \pi/2]$ (curve 1). However, at about a temperature $T = 0.637|J|$ a pair of local extrema is born inside the open interval $(0, \pi/2)$. This moment is fixed by the curve 2 in Fig. 6, right. With a further decrease in temperature, the minimum of this pair goes down and at $T_{c,0} = 0.63329|J|$ it

reaches the level of post-measurement entropy at $\theta = 0$ (curve 3). At this critical temperature, the optimal measurement angle ϑ suddenly switches from zero to the second minimum at $\vartheta = 0.64026 \approx 36.7^\circ$; see Fig. 7. The value of this new optimal measurement angle ϑ is found from the equation (see Refs. [31, 32])

$$\tilde{S}_0(T, B) = \tilde{S}_\vartheta(T, B). \quad (50)$$

This equation defines the boundary $0'$, which is shown in Fig. 6, left. As the system cools further, the optimal measurement angle continuously increases towards $\pi/2$ as shown by curve 4 in Fig. 6, right (see also Fig. 7). This limit value of ϑ is reached at the temperature $T_{c,\pi/2} = 0.59669|J|$ where a new sudden transition occurs, now similar to the second order.

The dependence $\Delta(T)$ is still continuous, but now has a fracture at the critical temperature $T_{c,0} = 0.63329|J|$. Its behavior is depicted in Fig. 8, top. As a result, the first derivative of the work deficit with respect to temperature undergoes a finite jump at the critical point, as shown in Fig. 8, bottom. Thus, the described transition combines discontinuous and continuous behavior and is similar to the first-order phase transitions [43, 46].

V. CONTINUOUS TRANSITIONS OF QUANTUM DISCORD

The quantum discord (8) for the system under study is written as

$$Q(T, B) = \min_{\theta} Q(\theta; T, B), \quad (51)$$

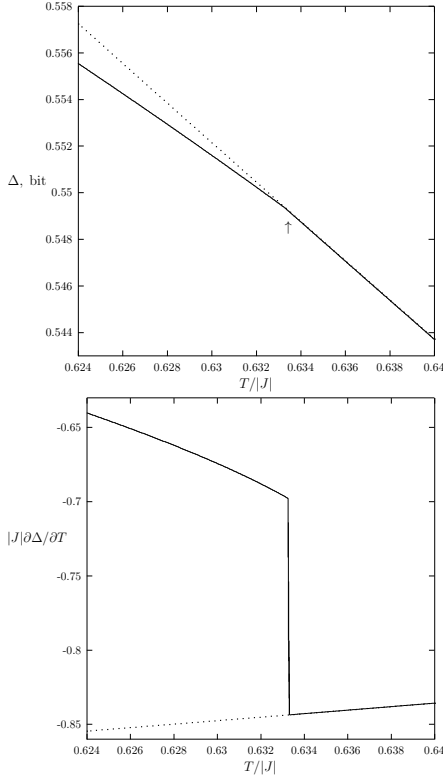


FIG. 8: Optimal one-way work deficit Δ (top) and its temperature derivative (bottom) versus $T/|J|$ by $J_z/|J| = -1.5$ and $B/|J| = 1.9$. The vertical arrow points the position of the fracture on the work deficit curve at $T/|J| = 0.63329$. The dotted lines correspond to the Δ_0 branch and are shown for comparison.

where $\mathcal{Q}(\theta; T, B)$ is an non-optimized discord, which is expressed in terms of Eqs. (5) and (9) as follows

$$\mathcal{Q}(\theta; T, B) = \bar{S}(\theta; T, B) - S(T, B) - (a+b) \ln(a+b) - (b+d) \ln(b+d). \quad (52)$$

It is clear that this quantity is related with non-optimized work deficit (30) by the equation

$$\begin{aligned} \mathcal{Q}(\theta; T, B) &= \Delta(\theta; T, B) - (a+b) \ln(a+b) \\ &- (b+d) \ln(b+d) + \frac{1+(a-d) \cos \theta}{2} \ln \frac{1+(a-d) \cos \theta}{2} \\ &+ \frac{1-(a-d) \cos \theta}{2} \ln \frac{1-(a-d) \cos \theta}{2}. \end{aligned} \quad (53)$$

Using the given equation it is easy to establish that quantum discord at zero optimal measurement angle, $Q_0(T, B) \equiv \mathcal{Q}(0; T, B)$, equals $\Delta_0(T, B)$ and can be written as

$$\begin{aligned} Q_0(T, B) &= \left[\frac{J}{T} \tanh \frac{J}{T} - \ln \left(\cosh \frac{J}{T} \right) \right] \\ &\times \left(1 + e^{J_z/T} \cosh \frac{B}{T} \operatorname{sech} \frac{J}{T} \right)^{-1}. \end{aligned} \quad (54)$$

The high-temperature expansion of this function is equivalent to the right-hand side of Eq. (33).

Similarly, the quantum discord at the second endpoint $\theta = \pi/2$ is given as

$$\begin{aligned} Q_{\pi/2}(T, B) &= a \ln a + d \ln d + (b+v) \ln(b+v) \\ &+ (b-v) \ln(b-v) - (a+b) \ln(a+b) - (b+d) \ln(b+d) \\ &- \frac{1+r}{2} \ln \frac{1+r}{2} - \frac{1-r}{2} \ln \frac{1-r}{2}, \end{aligned} \quad (55)$$

where $r = \sqrt{(a-d)^2 + 4v^2}$ equals (35) and a , b , and d are defined by Eq. (16). High-temperature behavior is now follow to

$$Q_{\pi/2}(T, B)|_{T \rightarrow \infty} = \frac{J^2 + J_z^2}{8T^2} - \frac{J^2 J_z}{8T^3} + O(1/T^4). \quad (56)$$

Next, the second derivative of average conditional entropy with respect to the measurement angle at $\theta = 0$ is equal to

$$\begin{aligned} \bar{S}_0''(T, B) &= \frac{1}{Z} \left[\left\{ \left(\frac{B}{T} + \ln \frac{\exp((J_z - B)/T) + \cosh(J/T)}{\exp((J_z + B)/T) + \cosh(J/T)} \right) \sinh \frac{B}{T} \right. \right. \\ &+ \left. \left(\cosh \frac{B}{T} - e^{-J_z/T} \cosh \frac{J}{T} \right) \left[\frac{J_z}{T} - \ln \left(\cosh \frac{J}{T} \right) \right] \right\} e^{J_z/2T} \\ &- \frac{1}{2} e^{-J_z/2T} \left[\frac{(J_z + B)/T - \ln(\cosh(J/T))}{\exp((J_z + B)/T) - \cosh(J/B)} + \frac{(J_z - B)/T - \ln(\cosh(J/T))}{\exp((J_z - B)/T) - \cosh(J/B)} \right] \sinh^2 \frac{J}{T} \left. \right]. \end{aligned} \quad (57)$$

Its high-temperature expansion is given as

$$\begin{aligned} \bar{S}_0''(T, B)|_{T \rightarrow \infty} &= \frac{J_z^2 - J^2}{4T^2} \\ &+ \frac{5J^4 + 2B^2 J^2 - 3B^2 J_z^2 - 4J_z^2 J^2 - J_z^4}{48T^4} + O(1/T^5). \end{aligned} \quad (58)$$

In similar way,

$$\begin{aligned} \bar{S}_{\pi/2}''(T, B) &= 2 \frac{v^2}{r} \left[1 - \left(\frac{a-2b+d}{r} \right)^2 \right] \ln \frac{1+r}{1-r} \\ &+ \frac{1}{2} (a-d)^2 \left[2 - \frac{1}{1+r} \left(1 + \frac{a-2b+d}{r} \right)^2 \right. \\ &\left. - \frac{1}{1-r} \left(1 - \frac{a-2b+d}{r} \right)^2 \right] \end{aligned} \quad (59)$$

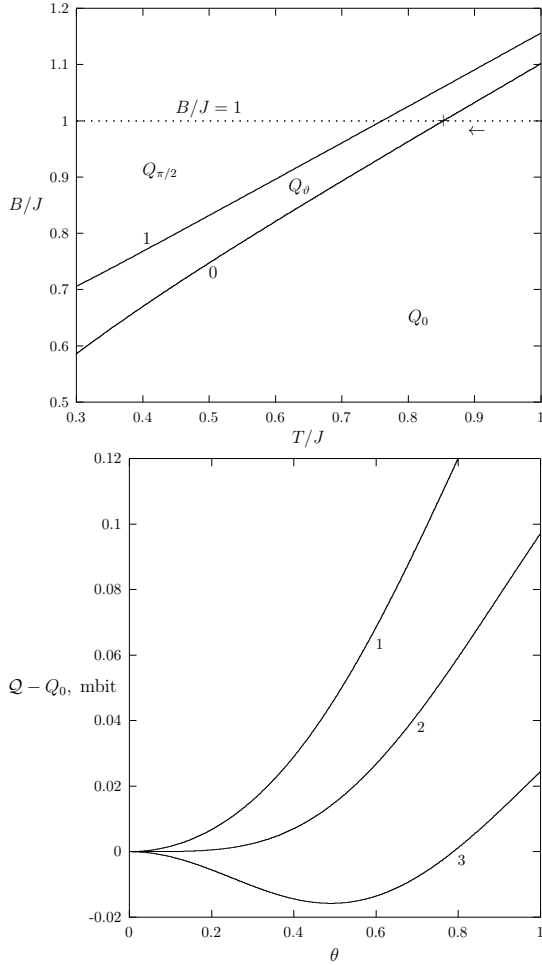


FIG. 9: (top panel) A fragment of (T, B) phase diagram for the quantum discord in the model with interaction constants $J = 1$ and $J_z = 1.02$. Solid lines 0 and 1 are the 0- and $\pi/2$ -boundaries, respectively. Dotted straight line is the trajectory of the system evolution, and arrow shows direction for such evolution. Symbol “+” has coordinates $(0.85361, 1)$ and marks the critical point. (bottom panel) Variation of non-optimized discord $\mathcal{Q} - Q_0$ versus measurement angle $\theta \in [0, 1]$ for temperatures $T/J = 0.88$ (1), 0.85361 (2), and 0.83 (3); $1 \text{ mbit} = 1 \times 10^{-3} \text{ bit}$.

and its asymptotics at high temperatures is given as

$$\bar{S}_{\pi/2}''(T, B)|_{T \rightarrow \infty} = \frac{J^2 - J_z^2}{4T^2} + O(1/T^4). \quad (60)$$

Equations for the 0- and $\pi/2$ -boundaries are similar to (39) and written as

$$\bar{S}_0''(T, B) = 0 \quad \text{and} \quad \bar{S}_{\pi/2}''(T, B) = 0. \quad (61)$$

Together with Eqs. (57) and (59) they allow to find the phase diagram of quantum discord.

If the optimal measurement angle ϑ changes continuously from zero to $\pi/2$, then this will be similar to the continuous (second-order) phase transitions of the Landau theory. It is remarkable that such situations do occur

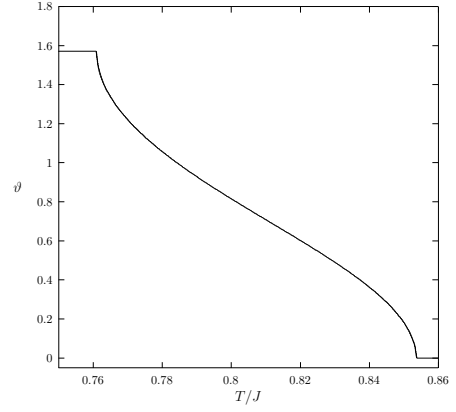


FIG. 10: Optimal measurement angle ϑ as a function of temperature by $J = 1$, $J_z = 1.02$, and $B/J = 1$. The Curie-like points are $T_{C,\pi/2}/J = 0.76106$ and $T_{C,0}/J = 0.85361$.

in the system under study. Indeed, consider the model with interaction constants $J = 1$ and $J_z = 1.02$. Numerically solving the above equations (61), we find the phase diagram shown in Fig. 9, top. Let the system evolve with a change in temperature along the path $B/J = 1$. During this evolution, the conditional entropy and therefore the non-optimized discord (which presented minus the constant part Q_0) qualitatively change their behavior, see Fig. 9, bottom. The function $\mathcal{Q}(\theta)$ monotonically increases at sufficiently high temperatures (curve 1 in Fig. 9, bottom) and its behavior near $\theta = 0$ is similar to $\sim \theta^2$. However, the behavior of this dependence changes qualitatively with approaching the 0-boundary (see Fig. 9, top) – its shape converts to $\sim \theta^4$ at the Curie-like point $T_{C,0} = 0.85361J$ (curve 2 in Fig. 9, bottom). Then, upon further cooling of the spin system, the minimum continuously shifts inside interval $(0, \pi/2)$; curve 3 in Fig. 9, bottom. This behavior near the point $T_{C,0}$ is well approximated by Landau-like expansion

$$\mathcal{Q}(\theta; T, B) - Q_0(T, B) \approx +\frac{1}{2!}\bar{S}_0''(T, B)\theta^2 + \frac{1}{4!}\bar{S}_0''''(T, B)\theta^4. \quad (62)$$

Here $Q_0(T, B)$ and $\bar{S}_0''(T, B)$ are given by Eqs. (54) and (57), respectively; expression for the fourth derivative, $\bar{S}_0''''(T, B)$, is too cumbersome and therefore we do not present it.

With decreasing temperature, the interior minimum tends continuously to the value $\theta = \pi/2$, which is attained at temperature $T_{C,\pi/2} = 0.76106J$, as depicted in Fig. 10. At this second Curie-type point, another second-order phase transition occurs. Below the temperature $T_{C,\pi/2}$, the optimal measurement angle again takes stationary value, now equal to $\pi/2$. Near the critical point $T_{C,0}$, the value $\vartheta(T)$ follows to law (47) and

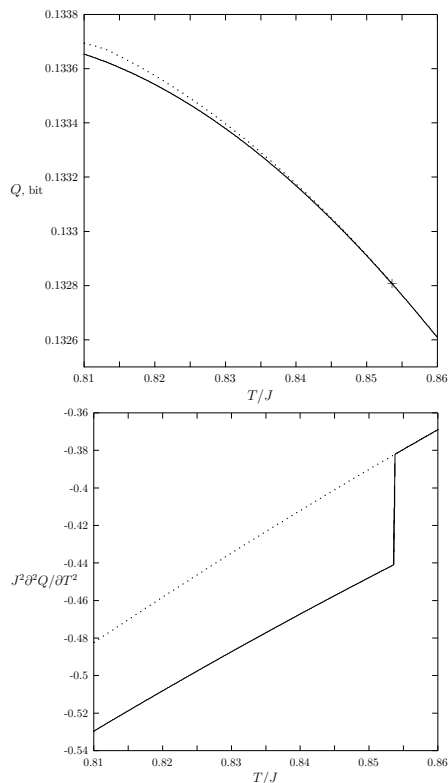


FIG. 11: Quantum discord Q (top) and its second derivative (bottom) near the Curie-like point $T_{C,0} = 0.85361J$ by $J = 1$, $J_z = 1.02$, and $B/J = 1$. Temperature dependencies of Q_0 (dotted lines) are shown for comparison. The “+” symbol has coordinates $(0.85361, 0.13281)$ and corresponds to the splitting point of the curves $Q(T)$ and $Q_0(T)$.

around $T_{C,\pi/2}$ changes as

$$\vartheta(T) = \begin{cases} \pi/2 - A \cdot (T - T_{C,\pi/2})^\beta, & \text{if } T > T_{C,\pi/2} \\ \pi/2, & \text{if } T \leq T_{C,\pi/2}, \end{cases} \quad (63)$$

where the critical exponent $\beta = 1/2$. So, near the critical points $T_{C,0}$ and $T_{C,\pi/2}$, the system experiences continuous sudden transitions. Here, quantum discord at any temperature $T \in [0, \infty)$ is a continuous and smooth function. However, its second-order derivatives with respect to temperature have finite jumps in both critical points. This is illustrated in Fig. 11 for the Curie-like point $T_{C,0}$. By analogy with the Ehrenfest classification, we assign these continuous transitions to sudden transitions/changes of the second order.

VI. CONCLUSIONS

It is well known that quantum correlations can be used to detect quantum phase transitions. For instance, the

next-nearest-neighbor entanglement has a maximum at the critical point in the one-dimensional transverse-field Ising system [47], entanglement shows scaling behavior in the vicinity of the transition point [48], bipartite entanglement indicates the quantum phase transitions in the frustrated spin models [49], Floquet dynamical phase transition is signaled by the behavior of entanglement spectrum [50].

To an even greater extent it manifests itself for quantum discord and information deficit. Using quantum discord, it was shown that the magnitude of quantum correlations increases in the region close to the critical points [51], and that it exhibits signatures of quantum phase transitions [52]. Moreover, the quantum discord makes it possible to confidently determine the points of the quantum phase transition at *finite* temperatures [53, 54]. (Using available solution for the XXZ chain in an external longitudinal field, the authors [54] also concluded, adding, however, numerical arguments, that the quantum discord of the two-site reduced density matrix does not contain regions with the variable optimal measurement angle; the question for the one-way quantum work deficit remains open.)

On the other hand, quantum correlations are considered as a physical resource (“as real as energy” [1]) and they themselves can undergo sudden changes. In Refs. [19, 20, 22], the sudden changes such as simple jumps (switches) from one stationary value of the optimal parameter to another without its continuous shift were studied in two-qubit systems.

In the present paper, we have shown that at the boundaries of regions with variable and constant optimal measurement angles, quantum discord exhibits a sudden change of second-order, while one-way quantum work deficit can experience sudden changes of both the first and second kinds. These phenomena shed additional light on the properties of nonclassical correlations in physical systems.

Our consideration is limited to the temperature dependencies of quantum correlations. It would be interesting to analyze similar dependencies on other control parameters, such as J , B , and J_z . These studies will probably require the use of catastrophe theory methods [44].

ACKNOWLEDGMENT

This work was supported by the program CITIS #AAAA-A19-119071190017-7.

- [1] R. Horodecki, P. Horodecki, M. Horodecki, and K. Horodecki, *Quantum entanglement*. Rev. Mod. Phys. **81**, 865 (2009).
- [2] K. Modi, A. Brodutch, H. Cable, T. Paterek, and V. Vedral, *The classical-quantum boundary for correlations: Discord and related measures*. Rev. Mod. Phys. **84**, 1655 (2012).
- [3] S. M. Aldoshin, E. B. Fel'dman, and M. A. Yurishchev, *Quantum entanglement and quantum discord in magnetoactive materials (Review Article)*. Fiz. Nizk. Temp. **40**, 5 (2014) [in Russian]; Low Temp. Phys. **40**, 3 (2014) [in English].
- [4] G. Adesso, T. R. Bromley, and M. Cianciaruso, *Measures and applications of quantum correlations (topical review)*. J. Phys. A: Math. Theor. **49**, 473001 (2016).
- [5] R. F. Werner, *Quantum states with Einstein-Podolsky-Rosen correlations admitting a hidden-variable model*. Phys. Rev. A **40**, 4277 (1989).
- [6] C. H. Bennett, D. P. DiVincenzo, J. A. Smolin, and W. K. Wootters, *Mixed-state entanglement and quantum error correction*. Phys. Rev. A **54**, 3824 (1996).
- [7] H. Ollivier and W. H. Zurek, *Quantum discord: a measure of the quantumness of correlations*. Phys. Rev. Lett. **88**, 017901 (2001).
- [8] W. H. Zurek, *Quantum discord and Maxwell's demons*. Phys. Rev. A **67**, 012320 (2003).
- [9] M. Horodecki, P. Horodecki, R. Horodecki, J. Oppenheim, A. Sen(De), U. Sen, and B. Synak-Radtke, *Local versus nonlocal information in quantum-information theory: Formalism and phenomena*. Phys. Rev. A **71**, 062307 (2005).
- [10] T. Ray, H. K. Sing, A. Isaacs, and W. F. Smith, *Infeasibility driven evolutionary algorithm for constrained optimization*. In: *Constraint-handling in Evolutionary Optimization*, edited by E. Mezura-Montes (Springer, Berlin, 2009), pp. 145-165.
- [11] M. A. Nielsen, *Quantum Information Theory*. PhD Dissertation, The University of New Mexico (1998); arXiv: quant-ph/0011036.
- [12] M. C. Arnesen, S. Bose, and V. Vedral, *Natural thermal and magnetic entanglement in the 1D Heisenberg model*. Phys. Rev. Lett. **87**, 017901 (2001).
- [13] T. Yu, J. H. Eberly, *Sudden death of entanglement*. Science **323**, 598 (2009).
- [14] F. Wang, P.-Y. Hou, Y.-Y. Huang, W.-G. Zhang, X.-L. Ouyang, X. Wang, X.-Z. Huang, H.-L. Zhang, L. He, X.-Y. Chang, and L.-M. Duan, *Observation of entanglement sudden death and rebirth by controlling a solid-state spin bath*. Phys. Rev. B **98**, 064306 (2018).
- [15] K. K. Sharma and V. P. Gerdt, *Entanglement sudden death and birth effects in two qubits maximally entangled mixed states under quantum channels*. Int. J. Theor. Phys. **59**, 403 (2020).
- [16] M. A. Yurishchev, *Quantum discord in spin-cluster materials*. Phys. Rev. B **84**, 024418 (2011).
- [17] S. Luo, *Quantum discord for two-qubit systems*. Phys. Rev. A **77**, 042303 (2008).
- [18] M. A. Yurischev, *Extremal properties of conditional entropy and quantum discord for XXZ, symmetric quantum states*. Quantum Inf. Process. **16**:249 (2017).
- [19] J. Maziero, L. C. Céleri, R. M. Serra, and V. Vedral, *Classical and quantum correlations under decoherence*. Phys. Rev. A **80**, 044102 (2009).
- [20] M. D. Lang and C. M. Caves, *Quantum discord and the geometry of Bell-diagonal states*. Phys. Rev. Lett. **105**, 150501 (2010).
- [21] J. P. G. Pinto, G. Karpat, and F. F. Fanchini, *Sudden change of quantum discord for a system of two qubits*. Phys. Rev. A **88**, 034304 (2013).
- [22] L. C. Céleri and J. Maziero, *The sudden change phenomenon of quantum discord*. In: *Lectures on General Quantum Correlations and Their Applications*, edited by F. F. Fanchini, D. O. Soares-Pinto, and G. Adesso (Springer, Berlin, 2017).
- [23] A. Bera, T. Das, D. Sadhukhan, S. S. Roy, A. Sen(De), and U. Sen, *Quantum discord and its allies: a review of recent progress*. Rep. Prog. Phys. **81**, 024001 (2018).
- [24] M. Ali, A. R. P. Rau, and G. Alber, *Quantum discord for two-qubit X states*. Phys. Rev. A **81**, 042105 (2010); Erratum in: Phys. Rev. A **82**, 069902(E) (2010).
- [25] X.-M. Lu, J. Ma, Z. Xi, and X. Wang, *Optimal measurements to access classical correlations of two-qubit states*. Phys. Rev. A **83**, 012327 (2011).
- [26] Q. Chen, C. Zhang, S. Yu, X. X. Yi, and C. H. Oh, *Quantum discord of two-qubit X states*. Phys. Rev. A **84**, 042313 (2011).
- [27] M. A. Yurischev, *Quantum discord for general X and CS states: a piecewise-analytical-numerical formula*. arXiv:1404.5735v1 [quant-ph].
- [28] M. A. Yurishchev, *NMR dynamics of quantum discord for spin-carrying gas molecules in a closed nanopore*. ZhETF **146**, 946 (2014) [in Russian]; J. Exp. Theor. Phys. **119**, 828 (2014) [in English]; arXiv:1503.03316v1 [quant-ph].
- [29] M. A. Yurischev, *On the quantum discord of general X states*. Quantum Inf. Process. **14**, 3399 (2015).
- [30] B.-L. Ye, Y.-K. Wang, , and S.-M. Fei, *One-way quantum deficit and decoherence for two-qubit X states*. Int. J. Theor. Phys. **55**, 2237 (2016).
- [31] M. A. Yurischev, *Bimodal behavior of post-measured entropy and one-way quantum deficit for two-qubit X states*. Quantum Inf. Process. **17**:6 (2018).
- [32] M. A. Yurischev, *Phase diagram for the one-way quantum deficit of two-qubit X states*. Quantum Inf. Process. **18**:124 (2019).
- [33] E. V. Moreva, M. Gramegna, and M. A. Yurischev, *On the possibility to detect quantum correlation regions with the variable optimal measurement angle*. Eur. Phys. J. D **73**:68 (2019).
- [34] A. Streltsov, H. Kampermann, and D. Bruss, *Linking quantum discord to entanglement in a measurement*. Phys. Rev. Lett. **106**, 160401 (2011).
- [35] N. Canosa, L. Ciliberti, and R. Rossignoli, *Quantum discord and information deficit in spin chains*. Entropy **17**, 1634 (2015), (Special issue: Quantum computation and information: Multi-particle aspects).
- [36] M. A. Nielsen and I. L. Chuang, *Quantum Computation and Quantum Information*. 10th anniversary edition (Cambridge University Press, Cambridge, 2010), Sec. 11.3.3.
- [37] W. H. Zurek, *Einselection and decoherence from an information theory perspective*. Ann. Phys. (Leipzig) **9**, 855 (2000).

- [38] L. Ciliberti, R. Rossignoli, and N. Canosa, *Quantum discord in finite XY chains*. Phys. Rev. A **82**, 042316 (2010).
- [39] Y. Huang, *Quantum discord for two-qubit X states: Analytical formula with very small worst-case error*. Phys. Rev. A **88**, 014302 (2013).
- [40] M. A. Yurischev, *Temperature-field phase diagrams of one-way quantum work deficit in two-qubit XXZ spin systems*. Quantum Inf. Process. **19**:110 (2020).
- [41] L. D. Landau, *K teorii fazovykh perekhodov*. I. ZhETF **7**, 19 (1937) [in Russian]; *Zur Theorie der Phasenumwandlungen II*. Phys. Zs. Sowjet. **11**, 26 (1937) [in German].
- [42] L. D. Landau and E. M. Lifshitz, *Statistical Physics*. Part 1 (Fizmatlit, Moscow, 2005) [in Russian]; (Pergamon, Oxford, 1980) [in English].
- [43] L. I. Klushin, A. M. Skvortsov, and A. A. Gorbunov, *An exactly solvable model for first- and second-order transitions*. Usp. Fiz. Nauk **168**, 719 (1998) [in Russian]; Phys.–Usp. **41**, 639 (1998) [in English].
- [44] V. I. Arnold, *Catastrophe Theory* (Nauka, Moskva, 1990) [in Russian], (Springer, Berlin, 1992) [in English].
- [45] G. Jaeger, *The Ehrenfest classification of phase transitions: Introduction and evolution*. Arch. Hist. Exact Sci. **53**, 51 (1998).
- [46] K. Binder, *Theory of first-order phase transitions*. Rep. Prog. Phys. **50**, 783 (1987).
- [47] T. J. Osborne and M. A. Nielsen, *Entanglement in a simple quantum phase transition*. Phys. Rev. A **66**, 032110 (2002).
- [48] A. Osterloh, L. Amico, G. Falci, and R. Fazio, *Scaling of entanglement close to a quantum phase transitions*. Nature **416**, 608 (2002).
- [49] G. Biswas and A. Biswas, *Entanglement in first excited states of some many-body quantum spin systems: indication of quantum phase transition in finite size systems*. Phys. Scr. **96**, 025003 (2021).
- [50] R. Jafari and A. Akbari, *Floquet dynamical phase transition and entanglement spectrum*. Phys. Rev. A **103**, 012204 (2021).
- [51] R. Dillenschneider, *Quantum discord and quantum phase transition in spin chains*. Phys. Rev. B **78**, 224413 (2008).
- [52] M. S. Sarandy, *Classical correlation and quantum discord in critical systems*. Phys. Rev. A **80**, 022108 (2009).
- [53] T. Werlang, C. Trippe, G. A. P. Ribeiro, and G. Rigolin, *Quantum correlations in spin chains at finite temperatures and quantum phase transitions*. Phys. Rev. Lett. **105**, 095702 (2010).
- [54] T. Werlang, G. A. P. Ribeiro, and G. Rigolin, *Spotlighting quantum critical points via quantum correlations at finite temperatures*. Phys. Rev. A **83**, 062334 (2011).